

---

# NOISE-AWARE TEXTURE-PRESERVING LOW-LIGHT ENHANCEMENT

---

A PREPRINT

**Zohreh Azizi**  
Media Communications Lab  
University of Southern California  
Los Angeles, CA, USA  
zazizi@usc.edu

**Xuejing Lei**  
Media Communications Lab  
University of Southern California  
Los Angeles, CA, USA  
xuejing@usc.edu

**C.-C. Jay Kuo**  
Media Communications Lab  
University of Southern California  
Los Angeles, CA, USA  
cckuo@sipi.usc.edu

September 4, 2020

## ABSTRACT

A simple and effective low-light image enhancement method based on a noise-aware texture-preserving retinex model is proposed in this work. The new method, called NATLE, attempts to strike a balance between noise removal and natural texture preservation through a low-complexity solution. Its cost function includes an estimated piece-wise smooth illumination map and a noise-free texture-preserving reflectance map. Afterwards, illumination is adjusted to form the enhanced image together with the reflectance map. Extensive experiments are conducted on common low-light image enhancement datasets to demonstrate the superior performance of NATLE.

**Keywords** low-light enhancement · retinex model · denoising

## 1 Introduction

Images captured in low-light conditions suffer from low visibility, lost details and high noise. Besides unpleasant human visual experience, low-light images can significantly degrade the performance of computer vision tasks such as object detection and recognition. As a result, low-light enhancement is widely demanded in consumer electronics and computer vision systems. Quite a few low light enhancement methods have been proposed. Early work is based on histogram equalization. Although being simple and fast, it suffers from unnatural color, amplified noise, and under/over-exposed areas. One popular approach for low-light enhancement is based on retinex decomposition. In this work, we propose to decompose the retinex model into the element-wise product of a piece-wise smooth illumination map and a noise-aware texture-preserving reflectance map, solve it with a simple and low complexity solution and, finally, use gamma correction to enhance the illumination map. We give the new method an acronym, "NATLE", due to its noise-aware texture-preserving characteristics.

Our main idea is sketched below. We begin with an initialization of a piece-wise smooth illumination map. Based on the retinex model and the initial illumination map, we can solve for the initial reflectance map. Afterwards, we apply nonlinear median filtering as well as linear filtering [1] to the RGB channels of initial reflectance map separately for noise-free, texture-preserving reflectance estimation. The complexity of our solution is low. Our work has several contributions. First, it conducts low light enhancement and denoising at the same time. Second, it has a low-complexity solution. Third, it preserves details without unrealistic edges for better visual quality.

The rest of this paper is organized as follows. Related work is reviewed in Sec. 2. Our new method is detailed in Sec. 3. Experimental results are shown in Sec. 4. Finally, concluding remarks and future work are given in Sec. 5.

## 2 Related Work

Motivated by the human vision system (HVS), retinex-based methods decompose an image into an element-wise product of a reflectance map and an illumination map and, then, adjust these two maps to enhance a low-light image. LR3M [2], which is a state-of-the-art retinex-based method, adopts an optimization framework that determines a piece-wise smooth illumination map and a noise-free contrast-enhanced reflectance map, denoted by  $L$  and  $R$ , respectively, for a low-light image. Although it yields a noise-free contrast-enhanced image, it suffers from unrealistic bold borders surrounded with white halo on edges (see Fig. 2e). Moreover, its run time is longer (see Table 1). STAR [3] is another low-light enhancement method based on the retinex model. It finds  $R$  and  $L$  using structure and texture maps extracted from the input image. Although STAR preserves texture well, it does not remove noise effectively. The Generative Adversarial Networks (GANs) offer another family of learning-based methods for low light enhancement. Examples include RDGAN [4] and EnlightenGAN [5]. RDGAN preserves texture well. Yet, its enhanced images tend to be noisy and with faded-color. EnlightenGAN can handle over-exposure without paired data, it tends to have noisy results as pointed out in [6]. Another CNN-based method, known as Zero-DCE [6], estimates enhancement curves for each pixel in an image.

## 3 Proposed NATLE Method

**System Overview.** The classic retinex model decomposes an observed image ( $S$ ) into an element-wise multiplication of its reflectance map ( $R$ ) and its illumination map ( $L$ ) as

$$S = R \circ L, \quad (1)$$

where  $R$  represents inherent features of the image, which is decoupled from lightness, and  $L$  delineates the lightness condition. A desired reflectance map includes texture and details while an ideal illumination map is a piece-wise smooth map indicative of the edge information. The NATLE method consists of two major steps:

- Step 1: Use the first optimization procedure to estimate  $L$ ;
- Step 2: Use the second optimization procedure to estimate  $R$  based on estimated  $L$  from Step 1.

Then, with gamma correction, NATLE yields the final output image. NATLE is summarized in Algorithm 1. Its intermediate processing results are illustrated in Fig. 1.

**Step 1.** To estimate  $L$ , we conduct the following optimization [2]:

$$\operatorname{argmin}_L \|L - \widehat{L}\|_F^2 + \alpha \|\nabla L\|_1, \quad (2)$$

where  $\alpha$  is a model parameter and  $\widehat{L}$  is an initial estimation of  $L$ . It is set to the default average of RGB three color components as  $\widehat{L} = 0.299R + 0.587G + 0.114B$ . The first term in the right-hand-side of Eq. (2) demands that  $L$  represents the luminance while the second term ensures that  $L$  is a piece-wise smooth map containing remarkable edges only. We have the following approximation for the second term:

$$\lim_{\epsilon \rightarrow 0^+} \sum_x \sum_{d \in \{h,v\}} \frac{(\nabla_d L(x))^2}{|\nabla_d \widehat{L}(x)| + \epsilon} = \|\nabla L\|_1, \quad (3)$$

where  $d$  is the gradient direction and  $v$  and  $h$  indicate the vertical and horizontal directions, respectively. Thus, Eq. (2) can be rewritten as

$$\operatorname{argmin}_L \|L - \widehat{L}\|_F^2 + \sum_x \sum_{d \in \{h,v\}} A_d(x) (\nabla_d L(x))^2, \quad (4)$$

where

$$A_d(x) = \frac{\alpha}{|\nabla_d \widehat{L}(x)| + \epsilon}. \quad (5)$$

**Step 2.** The reflectance map,  $R$ , can be solved with the following optimization:

$$\operatorname{argmin}_R \|R - \widehat{R}\|_F^2 + \beta \|\nabla R - G\|_F^2, \quad (6)$$

where  $\widehat{R}$  is a noise-free initialization of  $R$ :

$$\widehat{R} = S \oslash (L + \epsilon) - N, \quad (7)$$

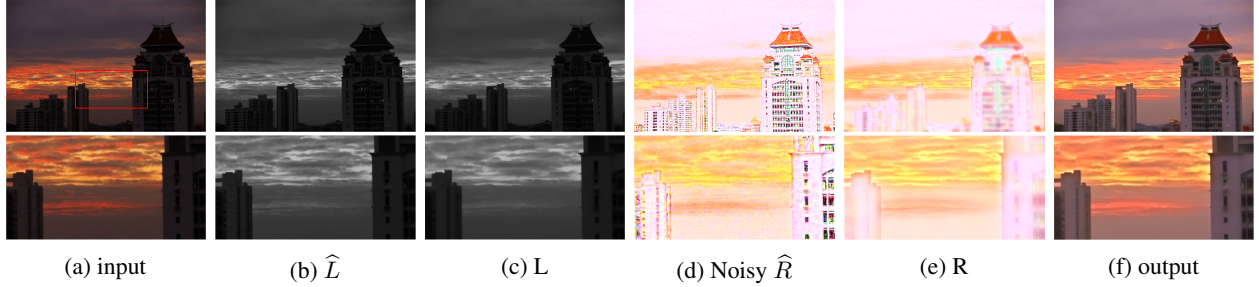


Figure 1: Illustration of NATLE’s processing steps: (a) input, (b) illumination map initialization, (c) illumination map estimation, (d) noisy reflectance map, (e) reflectance map estimation, (f) output after illumination gamma correction.

where  $S$  is the V channel of the input in the HSV color space,  $N$  is input noise,  $L$  is the estimated illumination obtained in Step 1,  $\oslash$  denotes the element-wise division and  $\varepsilon$  is a small value to prevent division by zero.

The first term in Eq. (6) is used to ensure: 1) the element-wise multiplication of  $R$  and  $L$  gives  $S$ , as demanded by the retinex model; 2)  $R$  is noise-free since  $\hat{R}$  is the element-wise division of  $S$  by  $L$  minus noise. Being inspired by [2], the second term in Eq. (6) has texture-preserving and noise-removal dual roles in our model. It enforces  $\hat{R}$  not to involve very small gradients to reduce noise. Yet, it is modified in our model to avoid bold borders between objects or halo next to edges, which appear in [2]. When  $\nabla S$  is small, [2] attempts to enhance the contrast by forcing  $\nabla R$  to be much larger than  $\nabla S$ ; however, it also affects edges that should not be amplified much, leading to unrealistic borders or halo near edges. In our model,  $\nabla R$  is forced to be slightly greater than  $\nabla S$  everywhere, except for very small gradients. This results in natural borders without halo as shown in Fig. 2. To this end, we modify  $G$  in [2] as

$$G = \begin{cases} 0, & \nabla S < \epsilon_g \\ \lambda \nabla S, & \text{otherwise} \end{cases} \quad (8)$$

where  $\epsilon_g$  is the threshold to filter out small gradients and  $\lambda$  controls the degree of amplification.

To obtain noise-free  $R$ , input noise  $N$  should be removed as shown in Eq. (7). To do so, we convert  $S \oslash (L + \varepsilon)$ , hue and saturation to the RGB color space and conduct denoising there. First, a median filter is applied to RGB channels to remove color impulse noise. Second, the Fast Adaptive Bilateral Filtering (fastABF) method [1] is used to remove remaining noise in each of RGB channels. FastABF employs the Gaussian kernel of different parameters at different pixel locations to adjust denoising degree according to the local noise level. Furthermore, it can be implemented by a fast algorithm. After denoising, the RGB output is converted back to the HSV space. Hue and saturation are saved for the final solution. The V channel serves as  $\hat{R}$  to initialize  $R$ . The above procedure not only remove noise in the V channel of noisy  $\hat{R}$  but also in hue and saturation channels.

It is worthwhile to point out that conventional high-performance denoising methods such as non-local-mean (NLM) [7] and BM3D [8] are slow in run time and weak in texture preservation. Faster denoising methods such as classic bilateral filtering [9] do not work well for images with heavy noise. The fastABF method is a good solution since it provides a good balance between low complexity, texture preservation and effective noise reduction.

**Closed-Form Solution.** The optimization problems in Eqs. (2) and (4) can be solved by differentiating with respect to  $L$  and  $R$  and setting the derivative to zero in a straightforward manner. There is no approximation neither high-complexity algorithm in order to solve them. Actually, the final solution can be derived in closed form as

$$l = (I + \sum_{d \in \{h,v\}} D_d^T \text{Diag}(a_d) D_d)^{-1} \hat{l}, \quad (9)$$

$$r = (I + \beta \sum_{d \in \{h,v\}} D_d^2)^{-1} (\hat{r} + \beta \sum_{d \in \{h,v\}} D_d^T g_d), \quad (10)$$

where  $\text{Diag}(y)$  is a diagonal matrix of vectorized  $y$  from matrix  $Y$ ,  $D_d$  is a discrete differential operator matrix that plays the role of  $\nabla$  and  $I$  is the identity matrix. Once vectors  $l$  and  $r$  are determined, they are reformed to matrices  $L$  and  $R$ , respectively. As the last step, gamma correction is applied to  $L$  to adjust illumination. The ultimate enhanced low-light image can be computed as

$$S' = R \oslash L^{\frac{1}{\gamma}}. \quad (11)$$

**Algorithm 1** Low-Light Enhancement Algorithm**Input:** Low-light Image

- 1: Illumination initialization;
- 2: Illumination estimation via Eq. (9);
- 3: Reflectance initialization via Eq. (7);
  - $S$  is the  $V$  channel of input in the HSV space;
  - Noisy  $\hat{R}$  with element-wise division ( $S/L$ );
  - Noisy  $\hat{R}$  back to the RGB space;
  - Apply median filtering and FastABF to RGB 3 channels;
  - Return to the HSV space:
    - $\hat{R}$  is the  $V$  channel;
    - Save denoised hue and saturation;
- 4: Reflectance estimation via Eq. (10);
- 5:  $S'$  is enhanced  $S$  via Eq. (11);
- 6: Integrate  $S'$ , hue & saturation and change to the RGB space

**Output:** Normal-light Image

## 4 Experiments

We conduct experiments on Matlab R2019b with an Intel Core i7 CPU @2.7GHz. The parameters  $\alpha$ ,  $\beta$ ,  $\lambda$  and  $\gamma$  are set to 0.015, 3, 1.1 and 2.2, respectively. We carry out performance comparison of several benchmarking methods with two sets of images: 1) 59 commonly used low-light images collected from various datasets for subjective evaluation and no-reference comparison; 2) 15 images from the LOL paired dataset for reference-based comparison.

**Objective Evaluation.** A no-reference metric, ARISMC [13], and a reference-based one, SSIM [14], are adopted for objective evaluation of several methods in Table 1. While ARISMC assesses quality of both luminance and chrominance, SSIM evaluates structural similarity with the ground truth. The run time is also compared in the table. LR3M has the best ARISMC performance. NATLE has the best SSIM performance and the second best ARISMC. Yet, LR3M demands 25 more times than NATLE.

Table 1: Objective performance evaluation

Method	ARISMC ↓	SSIM ↑	Run Time (sec.) ↓
BIMEF [15]	3.1543	0.5903	<b>0.27</b>
CRM [16]	3.1294	0.5366	0.32
MF [17]	3.1342	0.4910	0.96
PIE [10]	3.0636	0.5050	1.55
SRIE [11]	3.1416	0.4913	16.89
LR3M [2]	<b>2.7262</b>	0.4390	127
NATLE (Ours)	2.9970	<b>0.6193</b>	4.98

**Subjective Evaluation.** A qualitative comparison of our method with four benchmarking methods is shown in Fig. 2. For the first street image, PIE, SRIE and RetinexNet amplify noise in the low-light enhanced image. RetinexNet has unnatural color. LR3M has extra borders or halo next to edges. For the second lamp image, PIE and SRIE have either dark or noisy background. RetinexNet is noisy and over-exposed with unnatural texture and color. LR3M has false red borders around the lamp. For the third hills image, PIE and SRIE has low-light results. RetinexNet reveals square traces of BM3D denoising on trees and has unnatural color. LR3M removes all texture in mountains and generates an extra border between mountain and sky. For the last bird image, PIE and SRIE have low-light shadow areas. RetinexNet and LR3M generate black border around the bird. RetinexNet has unnatural color while LR3M loses feather texture and blurs shadow area. NATLE yields noise-free images with natural edges in these examples. It enhances light adequately and preserves texture well.

**Discussion.** It is worthwhile to highlight several characteristics of the proposed NATLE method.

*a) Denoising and Texture Preservation.* NATLE effectively removes noise without losing texture detail when being applied to a wide range of low-light images. The optimization in Eq. (6) demands the enhanced reflectance map to be

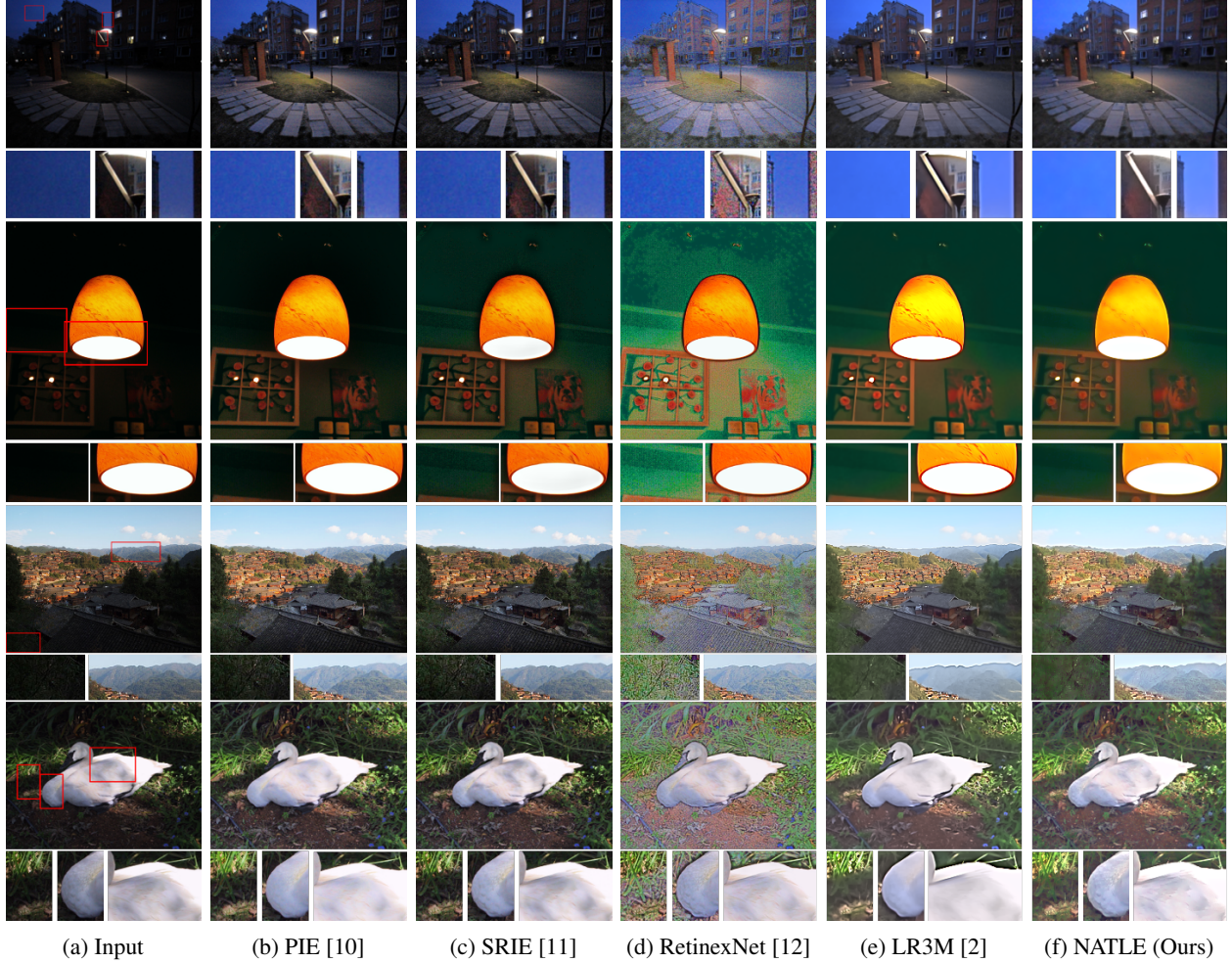


Figure 2: Qualitative comparison of low-light enhancement results.

as close as its noise-free form while preserving edges and textures in the input. As compared with [2], NATLE takes a moderate approach. That is, it does not denoise  $R$  more than needed. This is the main reason why NATLE can preserve texture, remove noise and maintain natural borders without halo at the same time.

*b) Speed.* NATLE performs fast and efficient with a closed-form solution. It is of low-complexity, since it does not demand iterations. It does not require sequential mathematical approximations, either. The performance of NATLE is affected by denoising methods. FastABF is chosen here. It is fine to adopt other denoising methods depending on the application requirement.

*c) Parameter Study.* The impact of model parameters  $\alpha$ ,  $\beta$ ,  $\lambda$  and  $\gamma$  is shown in Fig. 3. The results of setting  $\alpha = 0$  is shown in column (a). It removes the second term in Eq. (2), leading to a non-smooth illumination map and a noisy output. Moreover, removing this term results in color distortions such as the yellow area on grass beside the pavement at the bottom of the image. Column (b) shows results with  $\beta = 0$ . Without the second term in Eq. (6), edges and details are blurred. Column (c) is very noisy. It shows the need of denoising  $\hat{R}$ . Column (d) is the result by including all model parameters, which is clearly better than the other three cases.

## 5 Conclusion and Future Work

A low-light image enhancement method based on a noise-aware texture-preserving retinex model, called NATLE, was proposed in this work. It has closed-form solutions to the two formulated optimization problems and allows fast computation. Its superior performance was demonstrated by extensive experiments with both objective and subjective

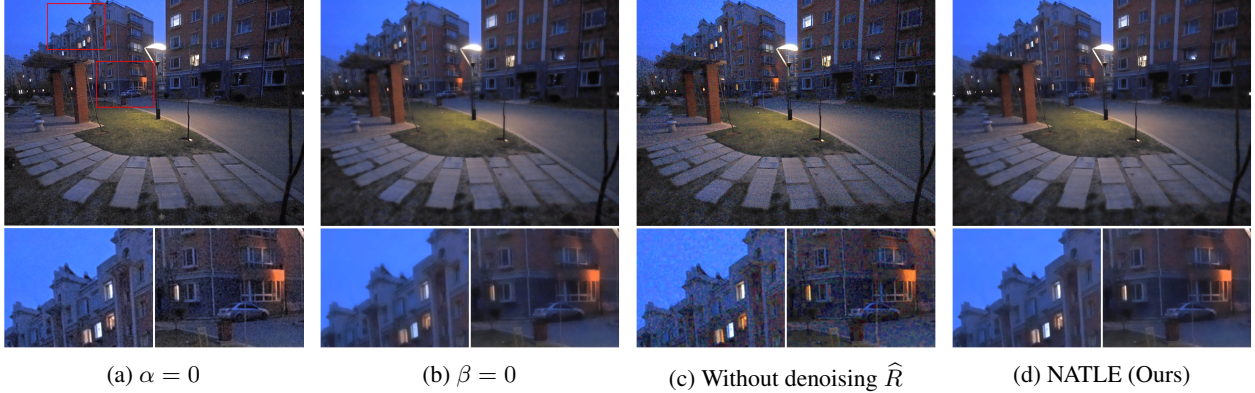


Figure 3: Parameter study for NATLE: (a) result with  $\alpha = 0$ , (b) result with  $\beta = 0$ , (c) result without denoising  $\hat{R}$ , (d) desired parameters.

evaluations. One possible future work is to extend this framework into video low-light enhancement. The main challenge is to preserve temporal consistency of enhanced video.

## References

- [1] R. G. Gavaskar and K. N. Chaudhury. Fast adaptive bilateral filtering. *IEEE Transactions on Image Processing*, 28(2):779–790, 2019.
- [2] X. Ren, W. Yang, W. Cheng, and J. Liu. Lr3m: Robust low-light enhancement via low-rank regularized retinex model. *IEEE Transactions on Image Processing*, 29:5862–5876, 2020.
- [3] J. Xu, Y. Hou, D. Ren, L. Liu, F. Zhu, M. Yu, H. Wang, and L. Shao. Star: A structure and texture aware retinex model. *IEEE Transactions on Image Processing*, 29:5022–5037, 2020.
- [4] J. Wang, W. Tan, X. Niu, and B. Yan. Rdgan: Retinex decomposition based adversarial learning for low-light enhancement. In *2019 IEEE International Conference on Multimedia and Expo (ICME)*, pages 1186–1191, 2019.
- [5] Yifan Jiang, Xinyu Gong, Ding Liu, Yu Cheng, Chen Fang, Xiaohui Shen, Jianchao Yang, Pan Zhou, and Zhangyang Wang. Enlightengan: Deep light enhancement without paired supervision. *arXiv preprint arXiv:1906.06972*, 2019.
- [6] Chunle Guo Guo, Chongyi Li, Jichang Guo, Chen Change Loy, Junhui Hou, Sam Kwong, and Runmin Cong. Zero-reference deep curve estimation for low-light image enhancement. In *Proceedings of the IEEE Conference on Computer Vision and Pattern Recognition (CVPR)*, pages 1780–1789, June 2020.
- [7] Antoni Buades, Bartomeu Coll, and Jean-Michel Morel. A non-local algorithm for image denoising. In *CVPR*, pages 60–65, 2005.
- [8] Kostadin Dabov, Alessandro Foi, Vladimir Katkovnik, and Karen Egiazarian. Image denoising with block-matching and 3D filtering. In *Image Process.: Algs. Sys., Neural Networks, and Machine Learning*, volume 6064, pages 354 – 365, 2006.
- [9] Volker Aurich and Jörg" Weule. Non-Linear Gaussian Filters Performing Edge Preserving Diffusion. In Gerhard Sagerer, Stefan Posch, and Franz Kummert, editors, *Musterverkennung 1995*, pages 538–545. Springer Berlin Heidelberg, 1995.
- [10] X. Fu, Y. Liao, D. Zeng, Y. Huang, X. Zhang, and X. Ding. A probabilistic method for image enhancement with simultaneous illumination and reflectance estimation. *IEEE Transactions on Image Processing*, 24(12):4965–4977, 2015.
- [11] X. Fu, D. Zeng, Y. Huang, X. Zhang, and X. Ding. A weighted variational model for simultaneous reflectance and illumination estimation. In *2016 IEEE Conference on Computer Vision and Pattern Recognition (CVPR)*, pages 2782–2790, 2016.
- [12] Chen Wei, Wenjing Wang, Wenhan Yang, and Jiaying Liu. Deep retinex decomposition for low-light enhancement. *arXiv preprint arXiv:1808.04560*, 2018.

- [13] K. Gu, G. Zhai, W. Lin, X. Yang, and W. Zhang. No-reference image sharpness assessment in autoregressive parameter space. *IEEE Transion on Image Processing*, 24(10):3218–3231, 2015.
- [14] Zhou Wang, A. C. Bovik, H. R. Sheikh, and E. P. Simoncelli. Image quality assessment: from error visibility to structural similarity. *IEEE Transaction on Image Processing*, 13(4):600–612, 2004.
- [15] Zhenqiang Ying, Ge Li, and Wen Gao. A bio-inspired multi-exposure fusion framework for low-light image enhancement. *ArXiv*, abs/1711.00591, 2017.
- [16] Z. Ying, G. Li, Y. Ren, R. Wang, and W. Wang. A new low-light image enhancement algorithm using camera response model. In *2017 IEEE International Conference on Computer Vision Workshops (ICCVW)*, pages 3015–3022, 2017.
- [17] Xueyang Fu, Delu Zeng, Yue Huang, Yinghao Liao, Xinghao Ding, and John W. Paisley. A fusion-based enhancing method for weakly illuminated images. *Signal Process.*, 129:82–96, 2016.